Sizing a battery-supercapacitor energy storage system with battery degradation consideration for high-performance electric vehicles

Tao Zhu[a,*], Roberto Lot[a,b], Richard G. A. Wills[a] and Xingda Yan[c]

[a]Department of Mechanical Engineering, University of Southampton, Southampton, SO17 1TU, UK.
[b]Department of Industrial Engineering, University of Padova, Padova, 35131, Italy
[c]Power engineer, Compound Semiconductor Applications Catapult, Newport, NP10 8BE, UK

ARTICLE INFO

Keywords:
Electric vehicle
Hybrid energy storage system
Battery degradation
Sizing
Energy Management

ABSTRACT

This paper presents sizing guides and energy management (EM) benchmarks of battery-supercapacitor (SC) hybrid energy storage system (HESS) in electric vehicle (EV) applications. We explain how to optimize the HESS size in order to minimize battery degradation and financial costs in EVs. We also illustrate the optimal EM benchmarks that can minimize battery degradation with whatever EM technique implemented. By decoupling the EM problem from the sizing one, we reveal the general trends of battery degradation with HESS size, which are irrelevant to design parameters of EVs and specifications of batteries and SCs. The vehicle-lifetime battery replacements and HESS costs are discussed with HESS sizing method. The efficacy of the proposed sizing guides and EM benchmarks is tested in the case study of a sports EV. Results show that the optimally sized HESS can extend battery lifetime by 37% as compared with the battery-only energy storage system and can reduce vehicle-lifetime HESS costs by up to 39% as compared with the unoptimized HESS designs, respectively.

Nomenclature

I. Symbols

A_h	ampere-hour throughput
C	ampere-hour capacity
$Cost$	cost
D	driving distance
E	energy capacity
I	current
J	objective function
J'	sub-objective function
k	execution stage
N	times of battery replacements
P	power
$\bar{P}$	mean power
$Price$	price
SOE	state of energy
T	temperature
t	time
U	voltage
u	decision variable
x	state variable
z	state transfer function
α	battery degradation coefficient
η	efficiency
ρ	power-to-energy density

II. Subscripts

BAT	battery pack
bus	power bus
$DCDC$	DC/DC converter
$HESS$	hybrid energy storage system
i	counter
$loss$	energy capacity loss (of battery pack)
max	maximum
nom	nominal
$rate$	current rate
SC	supercapacitor pack
veh	vehicle

*Corresponding author. Department of Mechanical Engineering, University of Southampton, Southampton, SO17 1TU, UK.
T.Zhu@soton.ac.uk (T. Zhu); roberto.lot@unipd.it (R. Lot); rgaw@soton.ac.uk (R.G.A. Wills); xingda.yan@csa.catapult.org.uk (X. Yan)
ORCID(s):

1. Introduction

Reducing environmental impact of private transportation is pushing increasing numbers of energy storage systems (ESSs) into vehicle drivetrains [1]. Batteries, as the primary energy storage in electric vehicles (EVs), are ideally suited to deliver energy for long-term vehicle propulsion, but they are not as suited to satisfy the short-term loads experienced in vehicle accelerations: to provide bursts of power in the seconds time frame over thousands of cycles [2, 3]. To fulfill high power pulses in vehicle propulsion, the battery-only ESS has to work at high current rates, which results in accelerated battery degradation [4, 5]. By incorporating supercapacitors (SCs) as power peaking units, the hybrid energy storage system (HESS) composed of batteries and SCs can substantially unload the power transients from batteries [6]. Compared with batteries, the reason for acceptance of SCs in an onboard HESS is their high pulse power capability, fast and efficient discharge and re-charging plus full charge cycling over 500,000 cycles [7]. The SCs essentially decouples the high transient power loads from batteries, which in return significantly relieves battery degradation [8, 9].

1.1. Literature review

The study of HESS involves complex, inter-related problems and objectives. From the engineering aspects, sizing and energy management (EM) are two research problems for optimization of objectives such as reducing the mass, initial costs, energy consumption or battery degradation [10]. Nevertheless, sizing and EM usually share overlapped objectives; for example, battery degradation or energy consumption is known as a combined result of both sizing and EM. Therefore, when investigating a single objective, previous research often establishes an "objective-oriented" integrated framework, co-solving both sizing and EM problems. For example, Mamun [11] develops a mathematical framework for combined sizing optimization and optimal EM of a series HEV with a HESS; by finding the optimal sizes of the battery pack and SC pack and the optimal power split strategies among power sources, the objective of energy consumption is minimized. Masih-Tehrani [12] develops a formulation for EM and sizing of a HESS in a series hybrid electric bus; with the objective of optimizing 10-years battery replacement cost due to battery degradation, the EM problem and sizing problem are solved by dynamic programming (DP) and genetic algorithm, respectively. Song [13] proposes an integrated optimization problem to solve the life cycle cost of a HESS in an electric city bus, in which the DP approach is responsible for searching the optimal HESS size while a rule-based controller is tuned to represent the near-optimal EM strategy. On the other hand, when solving a single problem like sizing, several co-existing objectives can be simultaneously investigated; therefore, previous research also performs "problem-oriented" multi-objective programming (MOP) optimization, co-investigating a few objectives. For example, Eldeeb [10] develops a MOP formulation to optimally size a HESS for a plug-in EV, where the four objectives of mass, volume, initial cost and battery degradation are minimized simultaneously. Song [14] adopts non-dominated sorting genetic algorithm II (NSGA-II) to size a HESS for use in an electric bus, while HESS initial cost and battery capacity loss are formulated as two conflicting objectives. Zhang [15] investigates the sizing problem of a HESS in an example EV and solves three objectives of battery state-of-health, HESS weight and initial cost by using wavelet-transform-based algorithm and NSGA-II. Targeted both objective- and problem-oriented investigation, the best practice of HESS study demonstrates a mixture of the integrated framework and MOP optimization. For example, Song [16] uses Pontryagin's minimum principle to determine not only the optimal EM strategy but also the best-case size for a HESS equipped with a plug-in EV, while objectives of battery degradation, fuel consumption and electricity consumption are optimized all together. Aiming at optimizing HESS mass and battery cycle life simultaneously, Shen [17] proposes a framework for EM and sizing of a HESS deployed in an electric passenger car, where the EM strategy is implemented by a rule-based controller while the optimal size is solved by dividing rectangles algorithm. Using DP approach, Song [18] formulates the optimization of battery degradation and electricity consumption of a HESS in EV applications, while the optimization problem is solved through the efforts of both EM and sizing; furthermore, sensitivity analysis is performed towards various temperatures and battery prices.

The sizing problem with the objective of reducing battery degradation has been widely studied by the abovementioned integrated framework or MOP optimization. However, these studies couple multiple problems or objectives but fail to induce the general relationship between HESS size and battery degradation, while the acquired sizing results are usually confined to specific case studies. With the integrated framework, it can offer a solution globally optimal to both sizing and EM. However, the optimality of the solution is subject to the specific EM controller implemented. For example, in [17] a rule-based controller is implemented along with optimizing HESS size; while in [10] an EM controller combing wavelet transformation and power split ratio is designed, using which the optimal sizing results are

acquired. These sizing results can only justify their optimality with the specifically implemented EM controller but cannot be proved optimal with another EM controller. Besides, since battery degradation is mostly formulated as a function of battery operating conditions (e.g., power, current, temperature) but has no direct connections with HESS size, battery degradation is mainly optimized by means of the EM controlling battery operating conditions, which means that the efforts to reduce battery degradation are more subject to EM but are rarely impacted by sizing [12]. With the MOP optimization, it can provide a set of non-inferior solutions (i.e. Pareto Frontier) for objectives from different metrics [14], while battery degradation is one of the objectives. However, its limitation is when generating the unique, optimal solution, it needs to coordinate different metrics by manually weighting each objective. For example, in [17] a weight factor is specified to make a tradeoff between HESS mass and battery degradation; the optimal solution is thus enabled, but the assignment of the weight factor is determined manually and thus has strong subjectivity. By assigning a high weight factor to the objective of battery degradation, the sizing results can be much near-optimal to battery degradation, but the results are still impacted by not only battery degradation but also the other objectives [15]. With either integrated framework or MOP optimization, the formulation of multiple problems or objectives is typically implicit and cannot be analyzed directly. The trends of battery degradation with HESS size can only be worked out for specific case studies after given the parameters of vehicle, battery and SC as well as running a large number of algorithms [18], but it is not sure if the trends can be generalized from the case study to wide scenarios using different vehicle specifications or EM techniques. Lastly, although the integrated framework or MOP optimisation can solve the optimal combination of HESS size and EM towards specific engineering requirements, however, when the requirements change, the optimal HESS size and EM also need to change. The EM is relatively easier to be updated, but once the vehicle is produced, the HESS size is difficult to alter because the size is something stationary and can hardly be relocated [19].

1.2. Contribution

Targeted the abovementioned limitations in previous research, this paper focuses on optimizing battery degradation of HESS by the sizing efforts, with the following contributions:

(1) By revealing the optimal EM scheme for a HESS to minimize battery degradation, the EM issue is decoupled from the sizing problem. The optimal EM scheme is not subject to specific EM technique and indicates how the power split strategies should perform to minimize battery degradation. For the case study in this paper, the optimal EM scheme is represented by the DP approach.

(2) Using the optimal EM scheme as a hypothesis, the general trends of battery degradation with HESS size are deduced. The general trends are demonstrated without specifying any case-study parameters or prescribing any EM techniques; therefore, the general trends are applicable to wide cases using different types of vehicles, batteries, SCs and EM techniques. The general trends are verified by the case study.

1.3. Paper organization

The overview of the remaining sections is shown in Fig. 1 and explained as follows. The investigation of HESS sizing starts with formulating the sizing problem in Section 2. Since fulfilling vehicle propulsion is the prerequisite for HESS design [20], this paper connects the energy/power requests of vehicle propulsion with the power capability/energy capacity of the HESS and thus constrains the feasible set of HESS size. With the objective of optimizing battery degradation by sizing efforts, battery degradation is formulated as functions of HESS size. Rather than ending up with merely investigating battery degradation can be reduced to some degree by the efforts of sizing, this paper further formulates the engineering impacts of battery degradation as HESS costs over vehicle lifetime and battery replacements over vehicle lifetime. HESS costs are defined as the sum of battery price losses due to degradation plus the procurement costs of SCs and DC/DC converter, which is a metric of the overall financial costs of using a HESS [21]. Battery replacements are the metric relevant to the maintenance of battery pack since too many replacements would cause trouble to both vehicle users and manufacturers [22]. Before using the above formulations to solve any specific case study, the following Section 3 aims at finding out general rules for optimizing battery degradation with HESS sizing. The optimization of battery degradation is generalized from two aspects - EM and sizing, because battery degradation is a coupled result of both aspects [23]. From the aspect of EM, the optimal EM scheme for HESS to minimize battery degradation is deduced, which benchmarks the best-case battery degradation can be achieved by whatever EM technique. The optimal EM scheme is then used as a hypothesis to enable the decoupling of EM and sizing, by which the general trends of battery degradation with HESS size are revealed; therefore, battery degradation can be optimized from the sizing aspect by referring to the general trends. The optimal EM scheme and general trends

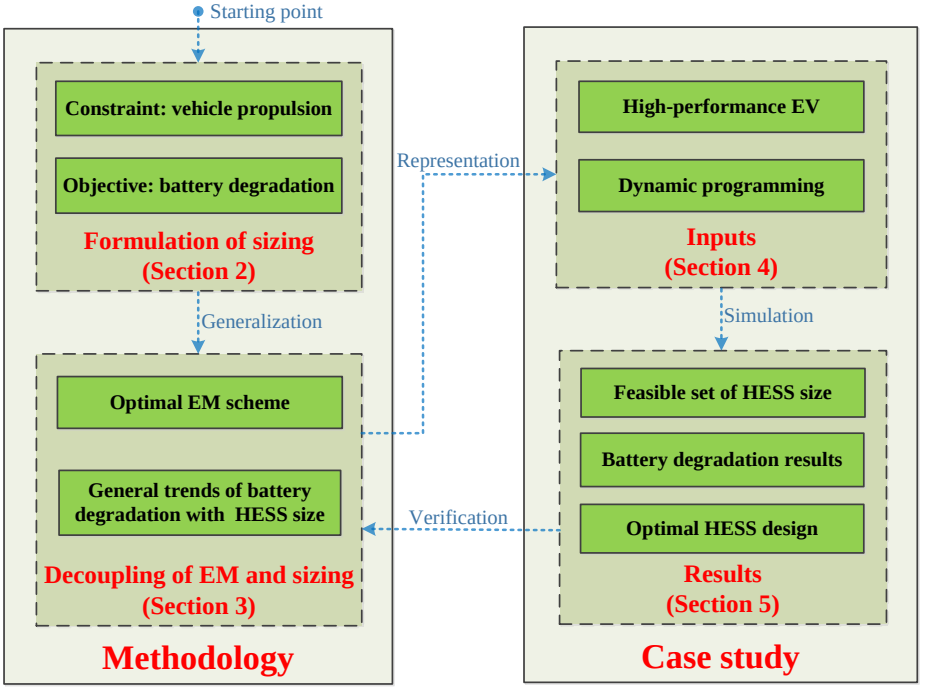

Figure 1: Schematic representation of the sizing methodology and case study.

are obtained from deductions so that their verification is necessary, and the verification is represented by a case study in Section 4. The case study uses a high-performance EV since this paper investigates the HESS sizing methodology for general EVs while emphasizes the application in high-performance EVs. As compared with standard EVs, high-performance EVs feature long-distance, aggressive driving capabilities [24], which requires to deploy a large battery pack working at high power/current rates and thus poses a possibility of severe battery degradation as well as subsequently frequent battery replacements and high degradation costs. Therefore, HESS sizing for high-performance EVs pursues more attention to battery degradation issues and challenges more the robustness of sizing methodology and thus needs specific investigation. To obtain case study results, the EM strategy of HESS is indispensable. However, the deduced optimal EM scheme is only benchmarks and cannot be used as a real EM strategy. In this case, the DP-based EM strategy is tailored to represent the optimal EM scheme. Afterward, Section 5 presents the simulation results, including the feasible set of HESS size, battery degradation data with HESS size and the optimal HESS design to minimize HESS costs. The simulation results are found following the deduced optimal EM scheme and general trends; consequently, the verification is done. Specifically, in Section 5.4, the underlying reasons for the influence of HESS size on HESS costs are discussed. Finally, Section 6 draws a conclusion.

2. General formulation of the sizing problem

The battery-SC HESS is considered to comprise of a battery pack, a SC pack and a DC/DC converter; thus sizing a battery-SC HESS is equivalent to identifying the combination of the sizes of above components [15]. Vehicle propulsion, which proposes specific power and energy requests, is the constraint for the sizing problem because fulfilling vehicle propulsion is the primary requirement for HESS [20]. Reducing battery degradation is the aim of sizing efforts as battery degradation can lead to a reduction of battery service time as well as significant financial costs [25]. However, battery degradation is just the sub-objective of the sizing problem; the battery replacements and HESS costs resulting from battery degradation are the final objectives because they are more straightforward metrics to evaluate the engineering impacts of battery degradation. Based on the above, the sizing problem can be expressed as: on satisfying vehicle propulsion requests, determine the sizes of battery pack, SC pack and DC/DC converter so that battery

replacements or HESS costs can reach a minimum via reducing battery degradation.

2.1. Constraints: power and energy requests from vehicle propulsion

EVs usually have an indicative driving range that accords with the usable energy capacity of onboard ESS [15]. To secure this driving range, the usable energy capacity of the whole HESS (battery pack + SC pack) is constrained by the vehicle energy consumption over driving range (E_{veh}). as Eq. (1), where E_{BAT} is the usable energy capacity of battery pack, E_{SC} is the usable energy capacity of SC pack.

$$E_{BAT} + E_{SC} \geq E_{veh} \tag{1}$$

Considering the SC pack is a power peaking device with tiny energy capacity (compared to the battery pack whose energy capacity is normally dozens of kWh, the SC pack is only hundreds of Wh) [13], E_{SC} can then be dismissed from Eq. (1) and E_{BAT} alone is expected to cover E_{veh}, as Eq. (2). Alternatively, taking into account the power to energy density of the battery (ρ_{BAT}, defined as battery maximum power capability $P_{BAT,max}$ divided by E_{BAT}) [26], this energy constraint can also be expressed with $P_{BAT,max}$.

$$\begin{cases} E_{BAT} \geq E_{veh} \\ \quad or \\ P_{BAT,max}/\rho_{BAT} \geq E_{veh} \end{cases} \tag{2}$$

Vehicle propulsion usually involves high-power operations such as sharp accelerations. To secure high-power operations, the maximum power capability of the whole HESS (battery pack + SC pack) is constrained by the maximum vehicle power request ($P_{veh,max}$), as Eq. (3), where $P_{SC,max}$ is the maximum power capability of SC pack. Alternatively, taking into account the power to energy density of the SC (ρ_{SC}, defined as $P_{SC,max}$ divided by E_{SC}) [27], this power constraint can also be expressed with E_{SC}.

$$\begin{cases} P_{BAT,max} + P_{SC,max} \geq P_{veh,max} \\ \quad or \\ P_{BAT,max} + E_{SC}\rho_{SC} \geq P_{veh,max} \end{cases} \tag{3}$$

After constraining the battery pack and SC pack, the DC/DC converter can be constrained by considering its maximum power capability ($P_{DCDC,max}$) as the same either with the SC pack if SC/battery topology is adopted (in this case, SC pack is interfaced by the DC/DC converter), or with the battery pack if battery/SC topology is adopted (battery pack is interfaced by the DC/DC converter) [28, 29].

2.2. Sub-objective: battery degradation coefficient or energy capacity loss as a function of HESS size

As aforementioned, DC/DC converter size is subject to the maximum power capability of either battery pack or SC pack; thus, DC/DC converter size is not used as an independent variable in the sizing problem. Namely, the HESS size is represented by the combination of battery pack size (scaled by E_{BAT}) and SC pack size (scaled by E_{SC}). Therefore, the sub-objective is battery degradation as a function of E_{BAT} and E_{SC}. Previous research [11] mainly adopts battery degradation coefficient (α, defined as the loss of usable energy capacity E_{loss} divided by original E_{BAT}) to scale battery degradation, as Eq. (4). The significance of α exists in its implication for battery replacements: the onboard battery pack needs to be replaced when α reaches 20% [10].

$$\alpha = E_{loss}/E_{BAT} \tag{4}$$

Apart from α, this paper also scales battery degradation by E_{loss}. Although E_{loss} can be transformed from α via Eq. (4), as E_{BAT} varies, the trend of E_{loss} is different from that of α (which is deduced in Section 3). The significance of E_{loss} exists in its implication for the financial losses due to degradation: the manufacturing price of battery is directly proportional to its energy capacity (e.g., battery unit price was imagined as 300 USD/kWh in 2017 [30]); thus, E_{loss}

responses to the losses of battery price. Based on the above, the sub-objective contains two parallel functions: one is α as a function of E_{BAT} and E_{SC}, and the other is E_{loss} as a function of E_{BAT} and E_{SC}, as Eq. (5).

$$\begin{cases} \alpha = f(E_{BAT}, E_{SC}) \\ \quad or \\ E_{loss} = g(E_{BAT}, E_{SC}) \end{cases} \tag{5}$$

2.3. Objective: battery replacements or HESS costs over vehicle lifetime as a function of HESS size

For long-term vehicle operations, as each time the onboard battery pack degrades to EOL, it needs to be replaced by a new one and simultaneously loses all its prices. Based on this, this paper scales the engineering impacts of battery degradation as battery replacements over vehicle lifetime (N) and battery price losses over vehicle lifetime ($Cost_{BAT}$), as Eqs. (6) and (7), respectively. The two equations use the α and E_{loss} in the time frame of one drive cycle to evaluate N and $Cost_{BAT}$ in the horizon of vehicle lifetime; an coefficient of 20% is divided by because battery EOL is commonly considered as α reaches 20% [10]; vehicle lifetime is considered to end when total mileage reaches 150000 km [31], while D_{veh} is the driving distance with one drive cycle, so that (150000km/D_{veh}) represents the transfer from one drive cycle to vehicle lifetime; $Price_{BAT}$ is battery manufacturing price (unit: USD/kWh). However, $Cost_{BAT}$ is not enough for assessing the overall financial costs of using a HESS: $Cost_{BAT}$ may be reduced by configuring a larger SC pack, but the procurement costs of a lager SC pack and the attached DC/DC converter are simultaneously higher [16]. In this case, this paper further defines HESS costs over vehicle time ($Cost_{HESS}$) as the sum of $Cost_{BAT}$, SC procurement costs ($Cost_{SC}$) and DC/DC converter procurement costs ($Cost_{DCDC}$), which is a comprehensive metric to assess the overall financial costs, as Eq. (8), where $Price_{SC}$ is SC manufacturing price (unit: USD/Wh) and $Price_{DCDC}$ is converter manufacturing price (unit: USD/kW).

$$N = \alpha/20\% \cdot 15000km/D_{veh} \tag{6}$$

$$Cost_{BAT} = E_{loss}/20\% \cdot 15000km/D_{veh} \cdot Price_{BAT} \tag{7}$$

$$Cost_{HESS} = Cost_{BAT} + Cost_{SC} + Cost_{DCDC} = Cost_{BAT} + E_{SC}Price_{SC} + P_{DCDC,max}Price_{DCDC} \tag{8}$$

Based on the above, the final objective contains two parallel functions: one is N as a function of E_{BAT} and E_{SC}, as Eq. (6), and the other is $Cost_{HESS}$ as a function of E_{BAT} and E_{SC}, as Eq. (8). The ultimate goal of the sizing problem is to find out the optimal combination of (E_{BAT}, E_{SC}), achieving minimum N or minimum $Cost_{HESS}$.

3. General trends of battery degradation with HESS size

Last section formulates battery degradation and its engineering impacts with HESS size. Before applying these formulations to any specific case study, this section aims at the general trends of battery degradation with HESS size. However, the EM technique of HESS is known to have a big impact on battery degradation: even with the same sized HESS, different EM techniques would lead to different degradation results [23]. To dismiss the impact of EM, this section initially reveals the optimal EM scheme to minimize battery degradation. The optimal EM scheme benchmarks the best-case battery degradation that can be ever achieved no matter what kind of EM technique is implemented, which further enables the decoupling of EM and sizing problems. Using the optimal EM scheme as a hypothesis, this section further deduces how α, E_{loss}, N and $Cost_{HESS}$ varies with E_{BAT} or E_{SC}.

3.1. Optimal EM scheme for a fix-sized HESS to minimize battery degradation

This subsection deduces how the battery operating power (P_{BAT}) and SC operating power (P_{SC}) should perform to optimally reduce E_{loss}. Since HESS size is fixed, minimizing E_{loss} can simultaneously minimize α, N and $Cost_{HESS}$.

Knowing that E_{loss} grows sharply with increasing P_{BAT} [32], the rate of E_{loss} ($\frac{dE_{loss}}{dt}$, defined as battery energy capacity loss in unit time) can be expressed as an increasing convex function of P_{BAT} [33], as Fig. 2, and Eq. (9) is workable, where $\bar{P}_{BAT}$ is the mean battery operating power.

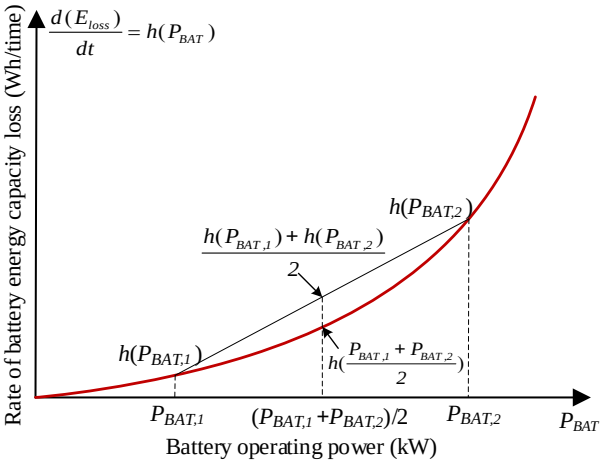

Figure 2: Rate of battery energy capacity loss as an increasing convex function of battery operating power.

$$\frac{h(P_{BAT,1}) + h(P_{BAT,2}) + ... + h(P_{BAT,n})}{n} \geq h(\frac{P_{BAT,1} + P_{BAT,2} + ... + P_{BAT,n}}{n}) = h(\bar{P}_{BAT}) \tag{9}$$

Assume the HESS operates following any given bus power profile (P_{bus}) from time zero to time t_n. At each time point ($t_i, i = 1, 2, ..., n$), the battery operating power ($P_{BAT,i}, i = 1, 2, ..., n$) is specifically allocated by the EM scheme. Based on Fig. 2 and Eq. (9), the E_{loss} over this period can be expressed as Eq. (10).

$$E_{loss} = \int_0^{t_n} \frac{dE_{loss}}{dt} dt = \int_0^{t_n} h(P_{BAT}) dt = \lim_{n\to\infty} \left[\sum_{i=1}^{n} h(P_{BAT,i})\right] \frac{t_n}{n} \geq \lim_{n\to\infty} h\left[\sum_{i=1}^{n} (P_{BAT,i}) \frac{1}{n}\right] t_n = h(\bar{P}_{BAT}) t_n \tag{10}$$

Eq. (10) implies that E_{loss} can get its minimum value $h(\bar{P}_{BAT})t_n$ by making P_{BAT} constant at $\bar{P}_{BAT}$. According to the "charge-sustaining principle" indicating that $\bar{P}_{BAT}$ approximately equals the mean bus power ($\bar{P}_{bus}$) [13], Eq. (10) can be transformed into Eq. (11).

$$E_{loss} \geq h(\bar{P}_{BAT}) t_n \approx h(\bar{P}_{bus}) t_n \tag{11}$$

Eq. (11) implies that the minimum value of E_{loss} approximately equals $h(\bar{P}_{bus})t_n$ and this value can be achieved by the optimal EM scheme allocating P_{BAT} constant at $\bar{P}_{bus}$. However, to maintain P_{BAT} constant at $\bar{P}_{bus}$, the optimal EM scheme must ensure that the residual power requests (P_{bus} - $\bar{P}_{bus}$) can be continuously compensated by the SC pack, which calls for configuring an ideal SC pack with excessively large energy capacity. In practice, a smaller SC pack would be configured but consequently, P_{BAT} cannot stay constant and would fluctuate around $\bar{P}_{bus}$ [34]. Towards practical application, the following adjusts the optimal EM scheme by deducing how P_{BAT} fluctuation impacts E_{loss} and raises the requirement for E_{SC}.

To make the deduction transparent, assume a bus power profile with only two points ($P_{bus,1}$ at t_1 and $P_{bus,2}$ at t_2), and the mean bus power is confirmed as $\bar{P}_{bus}$. To fulfill this profile, three alternative EM schemes are presented as ⓐ, ⓑ and ⓒ in Fig. 3. The P_{BAT} allocated by the three EM schemes are presented in Fig. 3 (I) and have different scales of fluctuation: ⓐ represents that P_{BAT} follows the bus power like a battery-only ESS and has large fluctuation; ⓒ represents that P_{BAT} stays constant at $\bar{P}_{bus}$ and has no fluctuation; ⓑ is a compromise between ⓐ and ⓒ, representing that P_{BAT} has medium fluctuation. The P_{BAT} of three EM schemes are then mapped to Fig. 3 (II), where the rate of E_{loss} is an increasing convex function of P_{BAT}, like Fig. 2; however, for the convenience of mapping, Fig. 3 (II) uses P_{BAT} as Y-axis. Based on Fig. 3 (II), the E_{loss} resulting from each EM scheme ($E_{loss,a}$, $E_{loss,b}$ and $E_{loss,c}$) can be expressed as Eq. (12) and compared as Eq. (13).

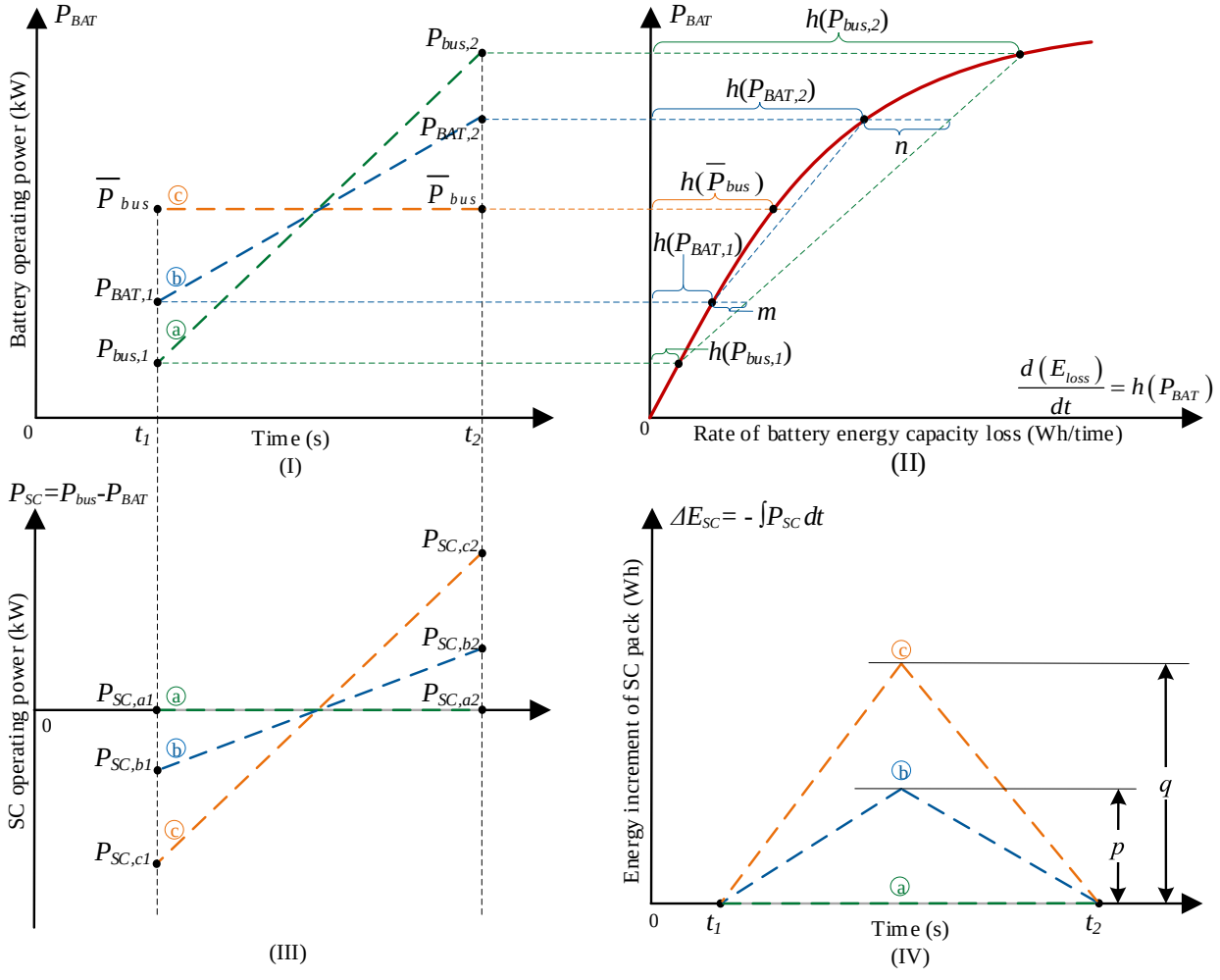

Figure 3: Three alternative EM schemes and their: (I) Battery operating power; (II) Rate of battery energy capacity loss as a function of battery operating power; (III) SC operating power; (IV) Energy increment of SC pack (a, b, c represent subscripts of three EM schemes; 1, 2 represent subscripts of two time points; m, n, p, q represent the algebraic length).

$$\begin{cases} E_{loss,a} = [h(P_{bus,1}) + h(P_{bus,2})]dt \\ E_{loss,b} = [h(P_{BAT,1}) + h(P_{BAT,2})]dt \\ E_{loss,c} = 2h(\bar{P}_{bus})dt \end{cases} \tag{12}$$

$$E_{loss,a} = E_{loss,b} + (m+n)dt > E_{loss,b} > E_{loss,c} \tag{13}$$

Eq. (13) indicates that the EM scheme with larger P_{BAT} fluctuation generates larger E_{loss}. Therefore, to reduce battery degradation, the EM scheme should aim at reducing P_{BAT} fluctuation, which requires assistance from the SC pack. Fig. 3 (III) presents the P_{SC} allocated by the three EM schemes, based on which, the energy increment of SC pack (ΔE_{SC}, defined as the time integral of P_{SC}) are worked out in Fig. 3 (IV). As the range of ΔE_{SC} equals the usable energy capacity of SC pack (E_{SC}), the E_{SC} required by each EM scheme ($E_{SC,a}$, $E_{SC,b}$ and $E_{SC,c}$) can be compared as Eq. (14), which indicates that E_{SC} is required to increase with smaller P_{BAT} fluctuation. If a SC pack

is configured according to the energy capacity required by EM scheme ⓑ, this SC pack can also fulfill ⓐ but cannot fulfill ⓒ. Thus, the potential for the EM to reduce P_{BAT} fluctuation is subject to the configured E_{SC}; as E_{SC} becomes larger, the EM scheme would have more flexibility to reduce P_{BAT} fluctuation, and as a result, reduce E_{loss}.

$$E_{SC,c} = q > E_{SC,b} = p > E_{SC,a} = 0 \tag{14}$$

3.2. The trend of battery degradation with SC pack size

This subsection regards E_{BAT} as fixed and investigates how α, E_{loss}, N and $Cost_{HESS}$ vary with E_{SC}. The deduction of optimal EM scheme already points out that E_{loss} decreases with growing E_{SC}; according to Eq. (4), α also decreases as E_{SC} grows; according to Eq. (6), N also decreases. According to Eq. (8), $Cost_{HESS}$ comprises $Cost_{BAT}$, $Cost_{SC}$ and $Cost_{DCDC}$. As E_{SC} grows, $Cost_{BAT}$ would decrease because E_{loss} can be reduced, while $Cost_{SC}$ and $Cost_{DCDC}$ would increase. In combination, the overall $Cost_{HESS}$ would depend on not only battery degradation but also the prices of battery, SC and DC/DC converter [12]. However, it can be inferred as a general trend independent of component prices that $Cost_{HESS}$ would initially drop but finally upswing with growing E_{SC}. This is because $Cost_{HESS}$ can be initially reduced with $Cost_{BAT}$ being effectively reduced by a lager E_{SC}; while the capability of enlarging E_{SC} to reduce $Cost_{BAT}$ would be increasingly less effective and finally reach to a limit after which $Cost_{BAT}$ along with battery degradation can hardly be further reduced but $Cost_{SC}$ and $Cost_{DCDC}$ would keep increasing as E_{SC} becomes larger. In combination of $Cost_{BAT}$, $Cost_{SC}$ and $Cost_{DCDC}$, there would be an extreme point of E_{SC} at which $Cost_{HESS}$ can be minimized.

3.3. The trend of battery degradation with battery pack size

This subsection regards E_{SC} as fixed and deduces how α, E_{loss}, N and $Cost_{HESS}$ vary with E_{BAT}. A battery degradation model to calculate α is introduced from [35], as Eq. (15). This model follows Arrhenius Law, using battery current rate (I_{rate}, unit: C), ampere-hour throughput (A_h) and ambient temperature (T, unit: Kelvin) as three independent variables, and a, b, c, d, e are five constants. A_h is defined as absolute battery operating current ($|I_{BAT}|$) multiplied by time t, and I_{rate} is $|I_{BAT}|$ divided by battery ampere-hour capacity (C_{BAT}), while C_{BAT} can be further expressed as E_{BAT} divided by battery nominal voltage ($U_{BAT,nom}$), as Eq. (16). Combining Eqs. (15) and (16), α can be expressed as a function of E_{BAT}, as Eq. (17), where a, b, c, d, e are substituted and T is set at the common temperature 20°C [36]. Since E_{BAT} is a variable representing battery pack size and independent of I_{BAT}, $U_{BAT,nom}$ and t, the partial derivative of α to E_{BAT} can be expressed as Eq. (18). The sign of Eq. (18) is always below zero so that α monotonously decreases with growing E_{BAT}. According to Eq. (6), N also decreases with growing E_{BAT}.

$$\alpha = (aT^2 + bT + c)exp[(dT + e)I_{rate}]A_h \tag{15}$$

$$\begin{cases} A_h = |I_{BAT}|t \\ I_{rate} = |I_{BAT}|/C_{BAT} \\ C_{BAT} = E_{BAT}/U_{BAT,nom} \end{cases} \tag{16}$$

$$\alpha = f(E_{BAT}) = 4.23 \cdot 10^{-4} exp\left(0.396 \frac{|I_{BAT}|U_{BAT,nom}}{E_{BAT}}\right)|I_{BAT}|t \tag{17}$$

$$\frac{\partial(\alpha)}{\partial(E_{BAT})} = f'(E_{BAT}) = -1.68 \cdot 10^{-4} exp\left(0.396 \frac{|I_{BAT}|U_{BAT,nom}}{E_{BAT}}\right) \frac{I_{BAT}^2 U_{BAT,nom}}{E_{BAT}^2} t < 0 \tag{18}$$

Combining Eqs. (4) and (17), E_{loss} can be expressed as a function of E_{BAT}, as Eq. (19). The partial derivative of E_{loss} to E_{BAT} can be expressed as Eq. (20). The sign of Eq. (20) depends on I_{rate}: if I_{rate} is less than 2.5C, Eq. (20)

would be above zero. This paper considers I_{rate} as less than 2.5C, because the batteries deployed in a HESS tend to be energy-intense batteries whose I_{rate} is usually smaller than 2C; moreover, with the help of SCs, the I_{rate} in practical operations can be secured far below 2.5C [26, 27]. Therefore, E_{loss} monotonously increases with growing E_{BAT}, and this trend can be explained from the engineering aspect, as follows. As E_{BAT} grows, more battery cells would be added as parallel branches into the battery pack, while the number of serial branches would maintain unchanged because the nominal voltage of battery pack ($U_{BAT,nom}$) is subject to the nominal bus voltage. Given the same operating power of battery pack (P_{BAT}), the battery cell in a larger battery pack would take on smaller operating power and current; therefore, the degradation of each battery cell can be lowered as represented by smaller energy capacity loss of each cell. However, the energy capacity loss of the whole battery pack (E_{loss}), which is the energy capacity loss of each battery cell added up, would increase. Finally, according to Eq. (8), $Cost_{HESS}$ also increases with growing E_{BAT}.

$$E_{loss} = E_{BAT}\alpha = g(E_{BAT}) = 4.23 \cdot 10^{-4} exp\Big(0.396\frac{|I_{BAT}|U_{BAT,nom}}{E_{BAT}}\Big)|I_{BAT}|E_{BAT}t \tag{19}$$

$$\begin{aligned}\frac{\partial(E_{loss})}{\partial(E_{BAT})} = g'(E_{BAT}) &= 4.23 \cdot 10^{-4} exp\Big(0.396\frac{|I_{BAT}|U_{BAT,nom}}{E_{BAT}}\Big)\Big(1 - \frac{0.396|I_{BAT}|U_{BAT,nom}}{E_{BAT}}\Big)|I_{BAT}|t \\ &= 4.23 \cdot 10^{-4} exp(0.396I_{rate})(1 - 0.396I_{rate})|I_{BAT}|t\end{aligned} \tag{20}$$

In summary of above deductions, Table 1 collects the general trends of battery degradation with HESS size, and these trends will be verified by a case study.

Table 1
General trends of battery degradation with battery pack size and SC pack size (α, battery degradation coefficient; E_{loss}, battery energy capacity loss; N, battery replacements over vehicle lifetime; $Cost_{HESS}$, HESS costs over vehicle lifetime; E_{BAT}, battery pack size; E_{SC}, SC pack size).

	α	E_{loss}	N	$Cost_{HESS}$
E_{BAT}	Negative	Positive	Negative	Positive
E_{SC}	Negative	Negative	Negative	Initially negative, finally positive

4. Case study

This section configures a case study of a high-performance EV to verify the optimal EM scheme and the deduced trends. DP approach is tailored to represent the optimal EM scheme for the case study. It searches for the optimal power split strategies to minimize battery degradation without involving the determination of HESS size; therefore, no matter what the HESS size is, the tailored DP approach can find out the optimal EM scheme fit for that specific HESS size [13]. Combining the DP-based optimal EM scheme and the general trends with HESS size, the globally optimal solutions can be worked out in terms of both EM and sizing.

4.1. Case study parameters

The case-study EV adopts Tesla Model S P85, which is a representative high-performance EV designed for fierce accelerations and long-distance driving, and its parameters can be found in [37, 38].

The HESS adopts a semi-active SC/battery topology, which is the most studied topology [28], as Fig. 4. By using a bidirectional DC/DC converter to interface the SC pack, the range of SC pack voltage can be made the most of. In this paper, the lower limit of SC pack voltage is set as 20% of the rated SC pack voltage, which means that the usable energy capacity of SC pack represents 96% of the rated energy capacity [39]. The batteries and SCs adopt Panasonic NCR18650B and Maxwell BCAP 3400 2.7V, respectively, and their specifications can be found in [40, 41] and [7]. The prices of the battery, SC and DC/DC converter are equal to 260 USD/kWh, 15 USD/kWh and 20 USD/kW [20, 25, 42], respectively.

The drive cycle is "Transformed US06 (T-US06)". Tailored for high-performance EVs, the T-US06 evolves from the standard US06 drive cycle that represents drastic driving conditions with high-speed operations and demanding

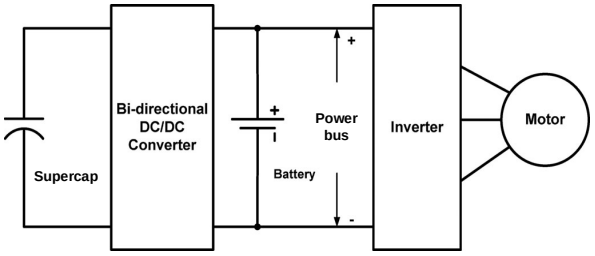

Figure 4: Semi-active SC/battery topology of HESS [28].

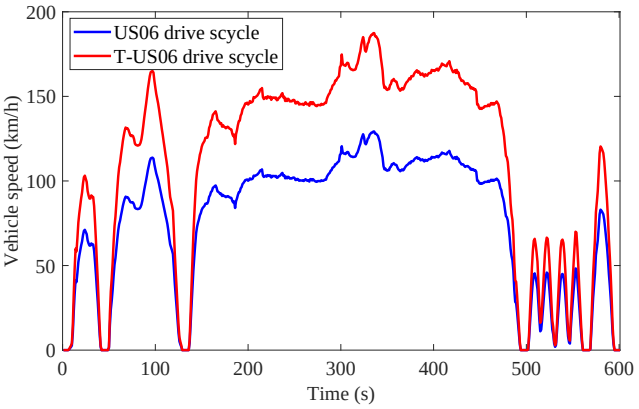

Figure 5: US06 and T-US06 drive cycles.

accelerations [43]. However, for the case-study vehicle with a motor power capability of 310 kW, the US06 cycle is still not drastic enough because this cycle merely proposes a maximum power request of 129kW. To design a more drastic drive cycle similar to US06, the T-US06 cycle keeps the timeline of US06 but multiplies the speed profile of US06 by 1.45, as compared in Fig. 5. Using T-US06 drive cycle, the maximum vehicle speed is 186 km/h and the maximum power request is 275 kW, which are very close to the vehicle's maximum potentials.

4.2. Optimal EM scheme based on DP approach

The DP approach is to split the bus power requests between the battery pack and SC pack, while its objective is to minimize N or $Cost_{HESS}$. It accepts prescribed case-study parameters as inputs, and then calculates the electrical characteristics of the battery pack, SC pack and DC/DC converter with time, using which to feed the objective functions and finally find out the optimal EM scheme. Its formulation is as follows.

(1) Execution stage (k), represents the timeline in the solving process. The duration of T-US06 drive cycle is 601 seconds so that 601 stages can be established with one second time step.

$$k = 1, 2, 3, ..., 601 \tag{21}$$

(2) Decision variable (u), is the controllable parameter which finding its values is the purpose of the EM efforts. Battery operating power P_{BAT} is adopted as the decision variable, and it is constrained by battery maximum power capability $P_{BAT,max}$, as Eq. (22). Given the bus power requests P_{bus}, the SC operating power P_{SC} can be determined by Eq. (23), where η_{DCDC} is DC/DC conversion efficiency and is a function of the current and voltage of SC pack [44].

$$\begin{cases} u_k = P_{BAT}(k) \\ |u_k| \leq P_{BAT,max} \end{cases} \tag{22}$$

$$P_{SC}(k) = \begin{cases} P_{bus}(k) - u_k \cdot \eta_{DCDC}, & P_{SC}(k) \geq 0 \\ P_{bus}(k) - u_k / \eta_{DCDC}, & P_{SC}(k) < 0 \end{cases} \tag{23}$$

(3) State variable (x), is the variable used to describe the mathematical "state" of the HESS. The state of energy (SOE, defined as the remaining energy divided by the rated energy capacity) of SC is used as the state variable, and it is constrained from 4% to 100% with 1% interval, according to the usable energy ratio 96%. Following the charge-sustaining principle [13], the final stage SOE is set the same with initial stage SOE at 50%.

$$\begin{cases} 4\% \leq x_k = SOE(k) \leq 100\% \\ x_{601} = x_1 = 50\% \end{cases} \tag{24}$$

(4) State transfer function (z), is the function connecting the state variables in adjacent stages; it represents how the iteration evolves and is a function of the control variable. Since the time step is one second, the state transfer function can be expressed as Eq. (25).

$$z_k = x_k - x_{k+1} = P_{SC}(k)/E_{SC} = [P_{bus}(k) - u_k]/E_{SC} \tag{25}$$

(5) The sub-objective (J') is to minimize either α or E_{loss} over a T-US06 drive cycle. Based on Eqs. (17) and (19), the sub-objective function can be expressed as Eq. (26), where $U_{BAT}(k)$ is battery operating voltage in stage k.

$$\begin{cases} MinJ' = Min\left\{\sum_{k=1}^{601} \alpha(k)\right\}, \quad \alpha(k) = 4.23 \cdot 10^{-4} exp\left(0.396 \frac{|u_k| U_{BAT,nom}}{E_{BAT} U_{BAT}(k)}\right) \frac{|u_k|}{U_{BAT}(k)} \\ \qquad or \\ MinJ' = Min\left\{\sum_{k=1}^{601} E_{loss}(k)\right\}, \quad E_{loss}(k) = 4.23 \cdot 10^{-4} exp\left(0.396 \frac{|u_k| U_{BAT,nom}}{E_{BAT} U_{BAT}(k)}\right) \frac{|u_k| E_{BAT}}{U_{BAT}(k)} \end{cases} \tag{26}$$

(6) The objective is (J) to minimize either N or $Cost_{HESS}$ over vehicle lifetime. Based on Eqs. (6) and (8), the objective function can be expressed as Eq. (27).

$$\begin{cases} MinJ = Min\left\{\sum_{k=1}^{601} N(k)\right\} = Min\left\{\sum_{k=1}^{601} \alpha(k)\right\} \frac{150000km}{D_{veh} 20\%} \\ \qquad or \\ MinJ = Min\left\{\sum_{k=1}^{601} Cost_{HESS}(k)\right\} \\ \qquad = Min\left\{\sum_{k=1}^{601} E_{loss}(k)\right\} \frac{price_{BAT} 150000km}{D_{veh}} + E_{SC} Price_{SC} + P_{DCDC,max} Price_{DCDC} \end{cases} \tag{27}$$

5. Results and discussion

This section presents the simulation results of the case study. A feasible set constraining HESS energy capacity is first presented. Four HESS designs and one battery-only ESS design, which differ from each other by either battery pack size or SC pack size, are selected and compared to verify the optimal EM scheme and the trends of battery degradation coefficient/energy capacity loss with HESS size. The battery replacements and HESS costs are discussed over vehicle lifetime. Specifically, the optimal HESS design is worked out in terms of minimizing HESS costs.

5.1. Feasible set constraining HESS energy capacity

Combining Eqs. (2) and (3), the HESS energy capacity is constrained by a feasible set in Fig. 6, where the usable energy capacity of battery pack (E_{BAT}) is the X-axis to represent battery pack size and the usable energy capacity of SC pack (E_{SC}) is the Y-axis to represent SC pack size. Any point within the feasible set can be a workable HESS design that meets the prescribed EV driving range and T-US06 drive cycle operations.

Five designs and their electrical configurations are labelled in Fig. 6, as points A, B, C, D and E. Points A and C are selected with the consideration of DC/DC conversion efficiency: in SC/battery HESS topology, the higher conversion

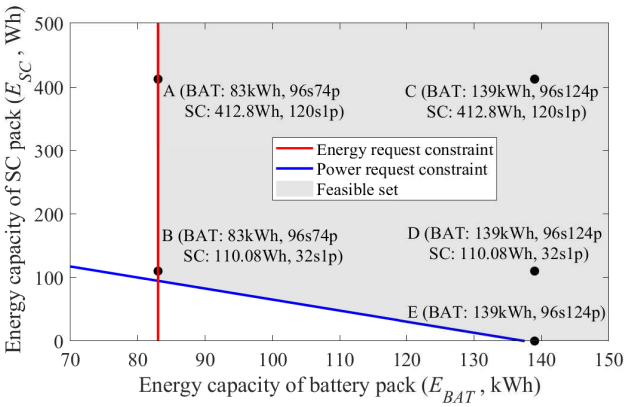

Figure 6: Feasible set constraining the energy capacity of HESS and five designs (A, B, C, D and E) with electrical configurations ("96s74p" means the pack has 96 serial cells and 74 parallel cells).

efficiency can be achieved with the narrower voltage gap between the SC pack and bus [42]. In this case, points A and C apply 120 SCs in series, respectively, reaching to a voltage level (324V) very close to the bus voltage (350V). In comparison, point A deploys the minimum allowable battery pack, while point C deploys a larger battery pack same as point E. Point B is selected near the joint of the power and energy constraints (rather than exactly on the joint, because in terms of battery packaging, the number of battery cells must be an integer while the joint is not the case). Point D has the same battery pack as E and the same SC pack as B. Point E is a battery-only ESS.

5.2. Verification of the optimal EM scheme

It is deduced that the optimal EM scheme depends on the SC pack size and a larger SC pack can enable the EM scheme to better reduce the fluctuation of battery operating power. To verify this, the simulated battery operating power (P_{BAT}) and SC operating power (P_{SC}) curves of the four HESS designs are compared in Fig. 7 (I) and (II), respectively; the variance of each curve, which is a sign of fluctuation, is also presented in the legends. Fig. 7 (I) shows that HESSs A and C have almost overlapped P_{BAT} curves and very close variances (so do HESSs B and D). This is because they have the same sized SC packs, which makes DP generate almost the same optimal EM schemes. The fluctuation of A or C is smaller than that of B or D, because A or C has a SC pack larger than that of B or D, which offers the EM scheme more flexibility to reduce the P_{BAT} fluctuation. Similarly, HESSs A and C have almost overlapped P_{SC} curves (so do HESSs B and D) in Fig. 7 (II). Based on Fig. 7, it is verified that the HESS design with a larger SC pack has more stabilized battery operating power; the HESS designs with the same sized SC pack have almost the same optimal EM scheme, while the size of battery pack only has a very limited impact on optimal EM scheme.

5.3. Verification of battery degradation coefficient and energy capacity loss with HESS size

Fig. 8 (I) and (II) compare the battery degradation coefficient (α) and energy capacity loss (E_{loss}) curves of the five designs, respectively; the final value of each curve is also presented in the legends. Fig. 8 (I) shows that HESS C has the smallest α among all designs because C has both the largest battery pack and the largest SC pack; HESS B has the largest α among the four HESS designs because B has both the smallest battery pack and the smallest SC pack. The α curve of A or D lies in the middle between B and C, because the battery pack and SC pack of A or D are smaller than those of C but larger than those of B. Fig. 8 (II) shows that HESS A has the smallest E_{loss} among all designs because A has both the smallest battery pack and the largest SC pack; HESS D has the largest E_{loss} among the four HESS designs because D has both the largest battery pack and the smallest SC pack. The battery-only ESS E has both the largest α and the largest E_{loss} due to no SC pack.

5.4. Discussion on battery replacements and HESS costs with HESS size

Fig. 9 (I) and (II) work out battery replacements over vehicle lifetime (N) and HESS costs over vehicle lifetime ($Cost_{HESS}$), respectively, as battery pack size varies from 80 to 170 kWh and SC pack size varies from 100 to 450 Wh.

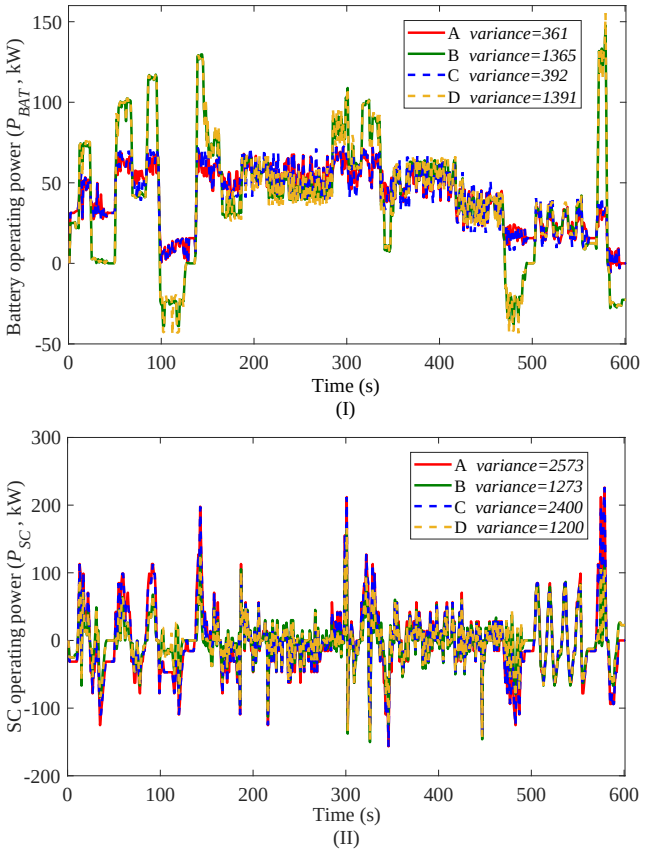

Figure 7: Verification of the optimal EM scheme by comparing the power curves of four HESS designs: (I) Battery operating power; (II) SC operating power, in time frame of one drive cycle.

Fig. 9 (I) indicates that the battery replacements are three to five times over vehicle lifetime, which is more than the normal situation in which the battery pack only needs one or even no replacement [33]. This is because the case study uses a high-performance EV running at a drastic drive cycle, which leads to the battery degrading much faster. Besides, battery replacements see a monotonous decline with increasing battery pack size and SC pack size. However, deploying a large battery pack and a large SC pack would require the consideration of their mass and volume, in case of the inconvenience to HESS packaging and chassis layout. Previous research [17, 45] tends to formulate the mass or volume as a weighted penalty function along with the main function of battery degradation, forming a MOP problem, which makes the sizing results impacted by not only battery degradation but also mass or volume. The mass and volume issues would not be further discussed since the main topic of this paper focuses on tailoring HESS size in terms of battery degradation.

Fig. 9 (II) shows that HESS costs vary with HESS size widely from 110000 to 180000 USD , which implies that a carefully sized HESS can significantly reduce the financial costs over vehicle lifetime. Furthermore, HESS costs witness a monotonous growth with increasing battery pack size. Thus, deploying an as small battery pack as possible is necessary to reduce HESS costs, while the minimum allowable battery pack size is constrained by vehicle propulsion requests. According to Fig. 6, the minimum allowable battery pack (i.e. the optimal battery pack) is 83 kWh. Besides, as SC pack size increases, HESS costs first drop and then rise, and the extreme point (i.e. the optimal SC pack) is 309.8 Wh. For the case study to minimize HESS costs, the optimal HESS design is to deploy a 83 kWh battery pack and a 309.8 Wh SC pack; the corresponding electrical configuration is 96 serial 74 parallel for the battery pack and 90 serial 1 parallel for the SC pack plus a 342 kW DC/DC converter. As compared with other feasible HESS designs in Fig. 9 (II), the optimal HESS can save financial costs by up to 39%.

To better understand the influence of HESS size on HESS costs, Fig. 10 (I) and (II) further discuss the underlying reasons for the trends in Fig. 9 (II).

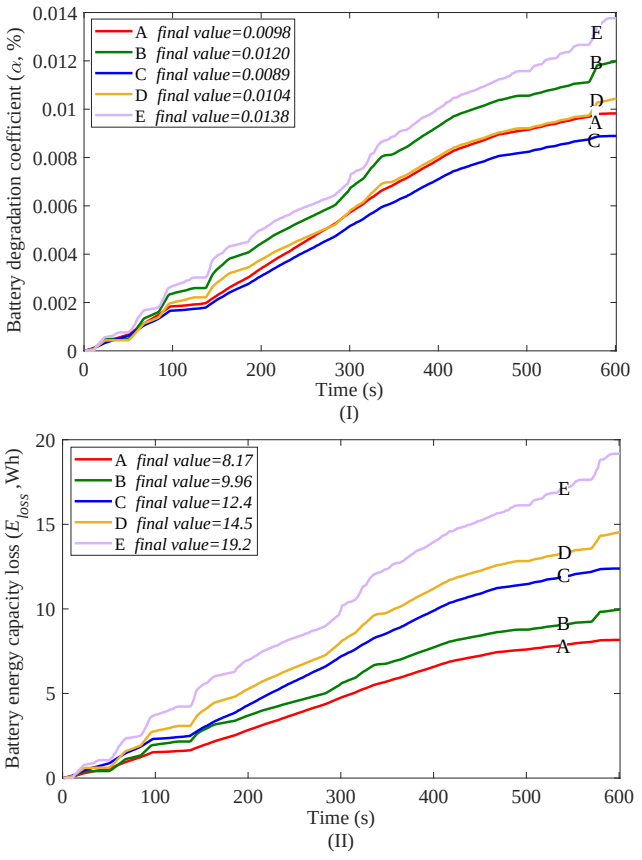

Figure 8: Verification of battery degradation with HESS size by comparing the degradation data of five ESS designs: (I) Battery degradation coefficient; (II) Battery energy capacity loss, in time frame of one drive cycle.

Fig. 10 (I) presents the overall HESS costs and sub-costs over vehicle lifetime, as SC pack size varies while battery pack size is held optimal at 83 kWh. Battery price losses ($Cost_{BAT}$) are the dominating part (around 90%) of HESS costs ($Cost_{HESS}$), while SC and DC/DC converter procurement costs ($Cost_{SC}$ and $Cost_{DCDC}$) only represent a small part. As SC pack size grows, $Cost_{BAT}$ witnesses a decelerating downtrend, which means that the efforts to reduce battery degradation by enlarging the SC pack become increasingly less effective. Meanwhile, $Cost_{SC}$ and $Cost_{DCDC}$ experience a near-linear uptrend. The overall $Cost_{HESS}$, as the sum of $Cost_{BAT}$, $Cost_{SC}$ and $Cost_{DCDC}$, initially decreases because $Cost_{BAT}$ can be significantly reduced, but finally rises up because $Cost_{BAT}$ is less effectively reduced with more SCs being deployed while $Cost_{SC}$ and $Cost_{DCDC}$ still increase rapidly. Therefore, an over large SC pack cannot contribute more to lowering overall costs.

Fig. 10 (II) presents the energy capacity loss of battery cell and battery pack after one drive cycle operation, as battery pack size varies while SC pack size is held optimal at 309.8 Wh. As battery pack size grows, the energy capacity loss of each battery cell can be reduced, because more parallel branches in the battery pack lead to each cell sharing smaller current and subsequently relieved degradation. However, the whole battery pack, with all the cells in combination, has increasing energy capacity loss with battery size increasing. Considering the battery price losses ($Cost_{BAT}$) resulting from energy capacity loss is the primary part of HESS costs ($Cost_{HESS}$), a larger battery pack with more energy capacity loss would have larger HESS costs.

6. Conclusion

This paper focuses on reducing battery degradation of a battery-SC HESS by the efforts of sizing and presents general sizing guides as well as EM benchmarks to optimize battery degradation. Battery degradation and its engineering impacts are formulated as functions of HESS size. The optimal EM scheme to reduce battery degradation is revealed,

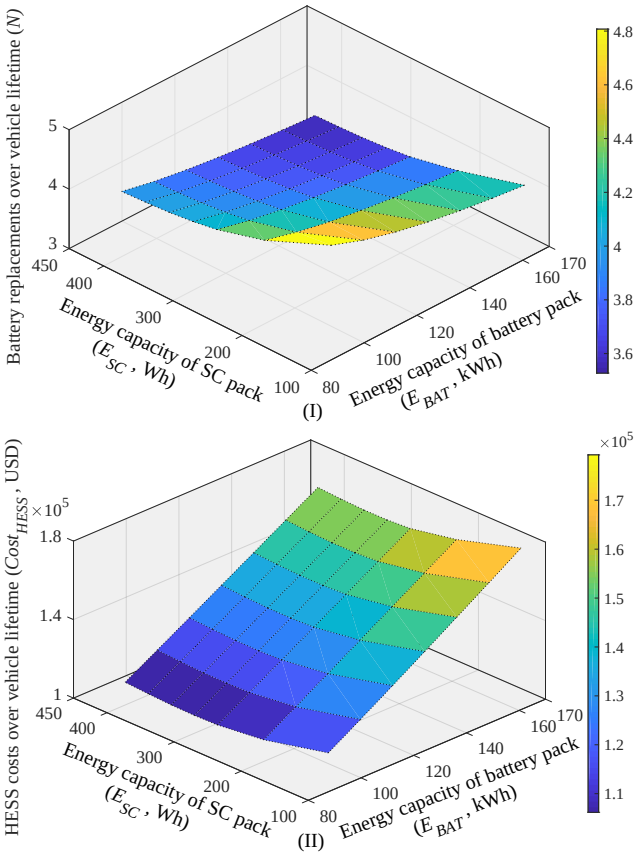

Figure 9: Discussion on the engineering impacts of battery degradation with HESS size : (I) Battery replacements over vehicle lifetime; (II) HESS costs over vehicle lifetime.

which indicates that the essence of reducing battery degradation exists in reducing the fluctuation of battery operating power; the optimal EM scheme is significantly affected by the size of SC pack but inapparently affected by the size of battery pack. Under the hypothesis that battery degradation can be best reduced following the optimal EM scheme, the general trends of battery degradation with HESS size are deduced as Table 1, which can be generalized to wide cases using different EM techniques, vehicles, batteries and SCs. A high-performance EV along with the DP-based EM approach is used as the case study, and five feasible HESS designs are compared to verify the optimal EM scheme and general trends. The battery replacements and HESS costs over vehicle lifetime, as the final objectives of the sizing problem, are discussed over the whole feasible set. Results show that the HESS with a larger battery pack and a larger SC pack can have fewer battery replacements; HESS costs grow with increasing battery pack size, while first drop and then rise with increasing SC pack size. The optimal HESS design for the case study to minimize HESS costs is solved as the combination of a 83 kWh battery pack, a 309.8 Wh SC pack and a 342 kW DC/DC converter. As a general guide to save financial costs over vehicle lifetime, it is suggested to deploy a HESS with an as small battery pack as constrained by vehicle driving range and a medium SC pack that can be found optimal at an extreme point.

Acknowledgements

The first author gratefully acknowledges the financial supports from China Scholarship Council and University of Southampton.

References

[1] B. Yang, T. Zhu, X. Zhang, J. Wang, H. Shu, S. Li, T. He, L. Yang, T. Yu, Design and implementation of battery/smes hybrid energy storage systems used in electric vehicles: A nonlinear robust fractional-order control approach, Energy (2019) 116510.

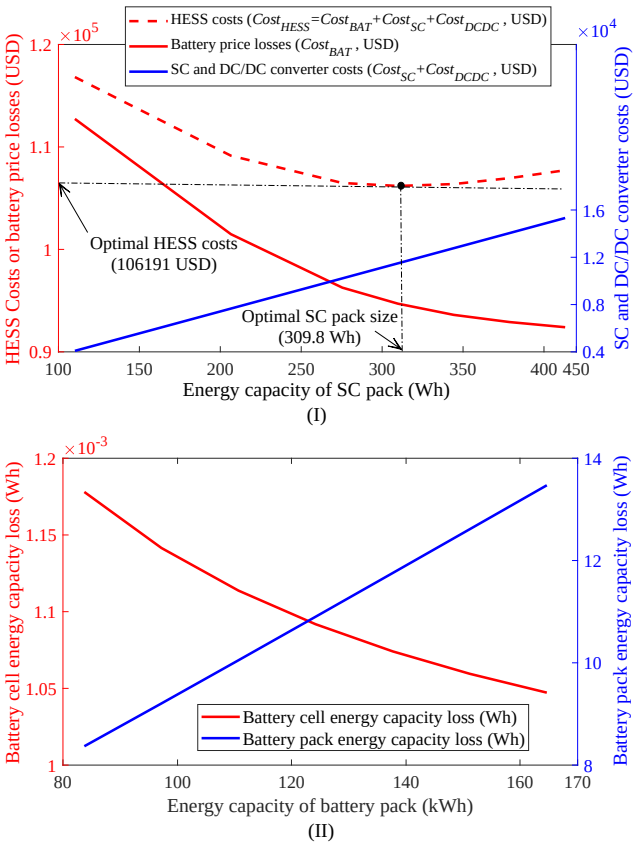

Figure 10: Further discussion on HESS costs with HESS size : (I) Overall HESS costs and sub-costs over vehicle lifetime, when SC pack size varies and battery pack size maintains optimal at 83 Wh; (II) Energy capacity loss of battery cell/battery pack after one drive cycle operation, when battery pack size varies and SC pack size maintains optimal at 309.8 Wh.

[2] P. Golchoubian, N. L. Azad, Real-time nonlinear model predictive control of a battery–supercapacitor hybrid energy storage system in electric vehicles, IEEE Transactions on Vehicular Technology 66 (2017) 9678–9688.

[3] Y. Wang, Z. Sun, Z. Chen, Development of energy management system based on a rule-based power distribution strategy for hybrid power sources, Energy 175 (2019) 1055–1066.

[4] S. Shili, A. Hijazi, A. Sari, X. Lin-Shi, P. Venet, Balancing circuit new control for supercapacitor storage system lifetime maximization, IEEE Transactions on Power Electronics 32 (2017) 4939–4948.

[5] G. He, Q. Chen, C. Kang, P. Pinson, Q. Xia, Optimal bidding strategy of battery storage in power markets considering performance-based regulation and battery cycle life, IEEE Transactions on Smart Grid 7 (2015) 2359–2367.

[6] A. Ostadi, M. Kazerani, A comparative analysis of optimal sizing of battery-only, ultracapacitor-only, and battery–ultracapacitor hybrid energy storage systems for a city bus, IEEE Transactions on Vehicular Technology 64 (2015) 4449–4460.

[7] Datasheet of maxwell 2.7v 3400f ultracapacitor cell, https://www.maxwell.com/images/documents/3V_3400F_datasheet.pdf/, 2018. Accessed on: Oct. 5, 2018.

[8] O. Gomozov, J. P. F. Trovão, X. Kestelyn, M. R. Dubois, Adaptive energy management system based on a real-time model predictive control with nonuniform sampling time for multiple energy storage electric vehicle, IEEE Transactions on Vehicular Technology 66 (2017) 5520–5530.

[9] S. Esmaeili, A. Anvari-Moghaddam, S. Jadid, Optimal operation scheduling of a microgrid incorporating battery swapping stations, IEEE Transactions on Power Systems 34 (2019) 5063–5072.

[10] H. H. Eldeeb, A. T. Elsayed, C. R. Lashway, O. Mohammed, Hybrid energy storage sizing and power splitting optimization for plug-in electric vehicles, IEEE Transactions on Industry Applications 55 (2019) 2252–2262.

[11] A. Mamun, Z. Liu, D. M. Rizzo, S. Onori, An integrated design and control optimization framework for hybrid military vehicle using lithium-ion battery and supercapacitor as energy storage devices, IEEE Transactions on Transportation Electrification 5 (2019) 239–251.

[12] M. Masih-Tehrani, M.-R. Ha'iri-Yazdi, V. Esfahanian, A. Safaei, Optimum sizing and optimum energy management of a hybrid energy storage system for lithium battery life improvement, Journal of Power Sources 244 (2013) 2–10.

[13] Z. Song, H. Hofmann, J. Li, X. Han, M. Ouyang, Optimization for a hybrid energy storage system in electric vehicles using dynamic programing approach, Applied Energy 139 (2015) 151–162.

[14] Z. Song, J. Li, X. Han, L. Xu, L. Lu, M. Ouyang, H. Hofmann, Multi-objective optimization of a semi-active battery/supercapacitor energy storage system for electric vehicles, Applied Energy 135 (2014) 212–224.
[15] L. Zhang, X. Hu, Z. Wang, F. Sun, J. Deng, D. G. Dorrell, Multiobjective optimal sizing of hybrid energy storage system for electric vehicles, IEEE Transactions on Vehicular Technology 67 (2018) 1027–1035.
[16] Z. Song, X. Zhang, J. Li, H. Hofmann, M. Ouyang, J. Du, Component sizing optimization of plug-in hybrid electric vehicles with the hybrid energy storage system, Energy 144 (2018) 393–403.
[17] J. Shen, S. Dusmez, A. Khaligh, Optimization of sizing and battery cycle life in battery/ultracapacitor hybrid energy storage systems for electric vehicle applications, IEEE Transactions on industrial informatics 10 (2014) 2112–2121.
[18] Z. Song, J. Li, J. Hou, H. Hofmann, M. Ouyang, J. Du, The battery-supercapacitor hybrid energy storage system in electric vehicle applications: A case study, Energy 154 (2018) 433–441.
[19] D. Luta, A. Raji, Optimal sizing of hybrid fuel cell-supercapacitor storage system for off-grid renewable applications, Energy 166 (2019) 530–540.
[20] J. Ruan, Q. Son, W. Yang, The application of hybrid energy storage system with electrified continuously variable transmission in battery electric vehicle, Energy (2019).
[21] C. Liu, Y. Wang, Z. Chen, Degradation model and cycle life prediction for lithium-ion battery used in hybrid energy storage system, Energy 166 (2019) 796–806.
[22] J. Li, A. M. Gee, M. Zhang, W. Yuan, Analysis of battery lifetime extension in a smes-battery hybrid energy storage system using a novel battery lifetime model, Energy 86 (2015) 175–185.
[23] Z. Song, H. Hofmann, J. Li, J. Hou, X. Han, M. Ouyang, Energy management strategies comparison for electric vehicles with hybrid energy storage system, Applied Energy 134 (2014) 321–331.
[24] M. Wieczorek, M. Lewandowski, A mathematical representation of an energy management strategy for hybrid energy storage system in electric vehicle and real time optimization using a genetic algorithm, Applied energy 192 (2017) 222–233.
[25] J. Liu, Z. Dong, T. Jin, L. Liu, Recent advance of hybrid energy storage systems for electrified vehicles, in: 2018 14th IEEE/ASME International Conference on Mechatronic and Embedded Systems and Applications (MESA), 2018, pp. 1–2. doi:10.1109/MESA.2018.8449191.
[26] E. Samadani, M. Mastali, S. Farhad, R. A. Fraser, M. Fowler, Li-ion battery performance and degradation in electric vehicles under different usage scenarios, International Journal of Energy Research 40 (2016) 379–392.
[27] L. Kouchachvili, W. Yaïci, E. Entchev, Hybrid battery/supercapacitor energy storage system for the electric vehicles, Journal of Power Sources 374 (2018) 237–248.
[28] J. Cao, A. Emadi, A new battery/ultracapacitor hybrid energy storage system for electric, hybrid, and plug-in hybrid electric vehicles, IEEE Transactions on power electronics 27 (2012) 122–132.
[29] Z. Song, J. Hou, H. F. Hofmann, X. Lin, J. Sun, Parameter identification and maximum power estimation of battery/supercapacitor hybrid energy storage system based on cramerâĂŞrao bound analysis, IEEE Transactions on Power Electronics 34 (2019) 4831–4843.
[30] T. Zhu, H. Min, Y. Yu, Z. Zhao, T. Xu, Y. Chen, X. Li, C. Zhang, An optimized energy management strategy for preheating vehicle-mounted li-ion batteries at subzero temperatures, Energies 10 (2017) 243.
[31] M. Carignano, V. Roda, R. Costa-CastellÃş, L. ValiÃśo, A. Lozano, F. Barreras, Assessment of energy management in a fuel cell/battery hybrid vehicle, IEEE Access 7 (2019) 16110–16122.
[32] J. Jaguemont, L. Boulon, P. Venet, Y. Dubé, A. Sari, Lithium-ion battery aging experiments at subzero temperatures and model development for capacity fade estimation, IEEE Transactions on Vehicular Technology 65 (2016) 4328–4343.
[33] C. Zhang, H. Min, Y. Yu, D. Wang, J. Luke, D. Opila, S. Saxena, Using cpe function to size capacitor storage for electric vehicles and quantifying battery degradation during different driving cycles, Energies 9 (2016) 903.
[34] T. Liu, H. Yu, H. Guo, Y. Qin, Y. Zou, Online energy management for multimode plug-in hybrid electric vehicles, IEEE Transactions on Industrial Informatics (2018) 1–1.
[35] J. Wang, J. Purewal, P. Liu, J. Hicks-Garner, S. Soukazian, E. Sherman, A. Sorenson, L. Vu, H. Tataria, M. W. Verbrugge, Degradation of lithium ion batteries employing graphite negatives and nickel–cobalt–manganese oxide+ spinel manganese oxide positives: Part 1, aging mechanisms and life estimation, Journal of Power Sources 269 (2014) 937–948.
[36] Z. Song, H. Hofmann, J. Li, J. Hou, X. Zhang, M. Ouyang, The optimization of a hybrid energy storage system at subzero temperatures: Energy management strategy design and battery heating requirement analysis, Applied energy 159 (2015) 576–588.
[37] M. Kardasz, M. Kazerani, Systematic electric vehicle scaling for test bed simulation, in: Transportation Electrification Conference and Expo (ITEC), 2016 IEEE, IEEE, 2016, pp. 1–6.
[38] O. Vynakov, E. Savolova, A. Skrynnyk, Modern electric cars of tesla motors company, Automation of technological and business-processes (2016) 9–18.
[39] H. Min, C. Lai, Y. Yu, T. Zhu, C. Zhang, Comparison study of two semi-active hybrid energy storage systems for hybrid electric vehicle applications and their experimental validation, Energies 10 (2017) 279.
[40] S. Kamalisiahroudi, J. Huang, Z. Li, J. Zhang, Study of temperature difference and current distribution in parallel-connected cells at low temperature, Int. J. Electr. Comput. Energ. Electron. Commun. Eng 8 (2014) 1471–1474.
[41] D. Wang, Y. Bao, J. Shi, Online lithium-ion battery internal resistance measurement application in state-of-charge estimation using the extended kalman filter, Energies 10 (2017) 1284.
[42] C.-M. Lai, Y.-H. Cheng, M.-H. Hsieh, Y.-C. Lin, Development of a bidirectional dc/dc converter with dual-battery energy storage for hybrid electric vehicle system, IEEE Transactions on Vehicular Technology 67 (2018) 1036–1052.
[43] C. Zheng, W. Li, Q. Liang, An energy management strategy of hybrid energy storage systems for electric vehicle applications, IEEE Transactions on Sustainable Energy 9 (2018) 1880–1888.
[44] W. Zhao, G. Wu, C. Wang, L. Yu, Y. Li, Energy transfer and utilization efficiency of regenerative braking with hybrid energy storage system,

Journal of Power Sources 427 (2019) 174–183.
[45] H. Yu, D. Tarsitano, X. Hu, F. Cheli, Real time energy management strategy for a fast charging electric urban bus powered by hybrid energy storage system, Energy 112 (2016) 322–331.